Journal of Breast Cancer

J Breast Cancer 2016 December; 19(4): 429-437 https://doi.org/10.4048/jbc.2016.19.4.429

ORIGINAL ARTICLE

Detectability and Usefulness of Automated Whole Breast Ultrasound in Patients with Suspicious Microcalcifications on Mammography: Comparison with Handheld Breast Ultrasound

Jae Jeong Choi, Sung Hun Kim[1], Bong Joo Kang[1], Byung Joo Song[2]

Department of Radiology, Dongtan Sacred Heart Hospital, Hallym University Medical Center, Hwaseong; Departments of [1]Radiology and [2]General Surgery, Seoul St. Mary's Hospital, The Catholic University of Korea College of Medicine, Seoul, Korea

Purpose: The purpose of this study was to prospectively evaluate the detectability and usefulness of automated whole breast ultrasound (AWUS) and to compare it with handheld breast ultrasound (HHUS) in cases with suspicious microcalcifications identified by mammography. **Methods:** Forty-two patients with 43 suspicious microcalcifications (25 malignant and 18 benign) detected by mammography underwent AWUS, HHUS, and histologic examination. With knowledge of the mammographic findings, HHUS was performed to assess the visibility of the microcalcifications and the presence of associated masses or ductal changes. Two radiologists reviewed the AWUS images in consensus using the same methods employed for HHUS. Detectability of AWUS was compared with that of HHUS and was correlated with histologic and mammographic findings. **Results:** Of the 43 lesions, 32 (74.4%) were detectable by AWUS and 31 (72.1%) by HHUS. No significant differences in sensitivity were found between the two methods ($p=0.998$). AWUS detected 96% (24/25) of malignant microcalcifications and 44.4% (8/18) of benign microcalcifications. AWUS was more successful in the detection of malignant vs. benign lesions (96.0% vs. 44.4%, $p=0.002$), lesions >10 mm vs. ≤10 mm in size (86.7% [26/30] vs. 46.2% [6/13], $p=0.009$), lesions with a fine pleomorphic or linear shape vs. a round or amorphous or coarse heterogeneous shape (94.7% [18/19] vs. 58.3% [14/24], $p=0.021$), and lesions associated with a mass or architectural distortion vs. without obvious changes on mammography (100% [19/19] vs. 54.2% [13/24], $p=0.022$). **Conclusion:** Detectability of AWUS was comparable to that of HHUS in cases where suspicious microcalcifications were identified on mammography. Therefore, AWUS might be helpful in the performance of ultrasound-guided percutaneous procedures for highly suspicious microcalcifications.

Key Words: *Breast neoplasms, Calcinosis, Mammary glands, Mammography, Ultrasonography*

INTRODUCTION

Mammography is a sensitive method for the detection of microcalcifications, which may be the only manifestation of early breast cancer [1-3]. Based on imaging characteristics, microcalcifications often cannot be classified as benign or malignant; in these cases, pathological examination by biopsy is recommended [3-6].

Recent advances in ultrasound (US) technology and the refinement of breast imaging techniques have enabled radiologists to evaluate breast microcalcifications. Several studies have reported that handheld breast US (HHUS) is useful in identifying malignant microcalcifications and provides effective guidance for percutaneous biopsy [7-12]. US-guided breast biopsy has several advantages over stereotactic biopsy, which include improved patient comfort, real-time visualization of needle placement, absence of radiation exposure, shorter duration of the procedure, and relatively low cost. However, most radiologists now performing breast US use handheld systems, which has some disadvantages because the scans are operator-dependent and therefore suffer from a lack of reproducibility.

Automated whole breast US (AWUS) scanners were originally designed to examine the entire breast and to overcome the operator dependency of HHUS [13,14]. Several studies have concluded that the sensitivity, diagnostic performances,

Correspondence to: **Sung Hun Kim**
Department of Radiology, Seoul St. Mary's Hospital, The Catholic University of Korea College of Medicine, 222 Banpo-daero, Seocho-gu, Seoul 06591, Korea
Tel: +82-2-2258-6253, Fax: +82-2-2258-1457
E-mail: rad-ksh@catholic.ac.kr

This works was supported from the Catholic Medical Center Research Foundation.

Received: June 21, 2016 **Accepted:** September 19, 2016

http://ejbc.kr | pISSN 1738-6756 eISSN 2092-9900

and image quality of AWUS and HHUS are equivalent [15-21]. However, these studies have primarily evaluated mass lesions in the breast. To date, there have been few studies evaluating AWUS findings for suspicious microcalcifications detected by mammography.

The purpose of this prospective study was to evaluate the ability of AWUS to detect suspicious microcalcifications originally identified by mammography, to characterize the lesion variables that affect their detectability, and to compare the effectiveness of AWUS with that of HHUS.

METHODS

Patients

Between March and August of 2012, 45 consecutive patients with mammographically detected suspicious microcalcifications, who were scheduled for US-guided or mammography-guided biopsy, were enrolled in our prospective study. Three of these patients were excluded because the biopsy was not performed. Thus, our study ultimately included 42 patients with 43 mammographically detected suspicious microcalcifications (Figure 1). The patients, who ranged in age from 28 to 80 years (average age, 53 years), underwent AWUS and HHUS examinations prior to their biopsy procedures. Six patients had a palpable lump in the breast. Institutional Review Board approval (KC12DSSI0235) and informed patient consent were obtained prior to the procedures.

All microcalcifications were sampled by US-guided 14-gauge core needle biopsy or mammography-guided (stereotactic) 11-gauge vacuum-assisted biopsy. If the microcalcifications were not visible by HHUS, stereotactic 11-gauge vacuum-assisted biopsy was performed. Two patients with microcalcifications visible by HHUS underwent stereotactic 11-gauge vacuum-assisted biopsy instead, because the extent of the lesion visualized by HHUS was much smaller than that visualized by mammography. A median number of seven core samples (range, 5–12) per biopsy were obtained by 14-gauge core needle biopsy and a median number of 14 core samples (range, 10–17) per biopsy were obtained by stereotactic 11-gauge vacuum-assisted biopsy. After five core samples were obtained by 14-gauge needle core biopsy and 10 core samples were obtained by 11-gauge vacuum-assisted biopsy, radio-

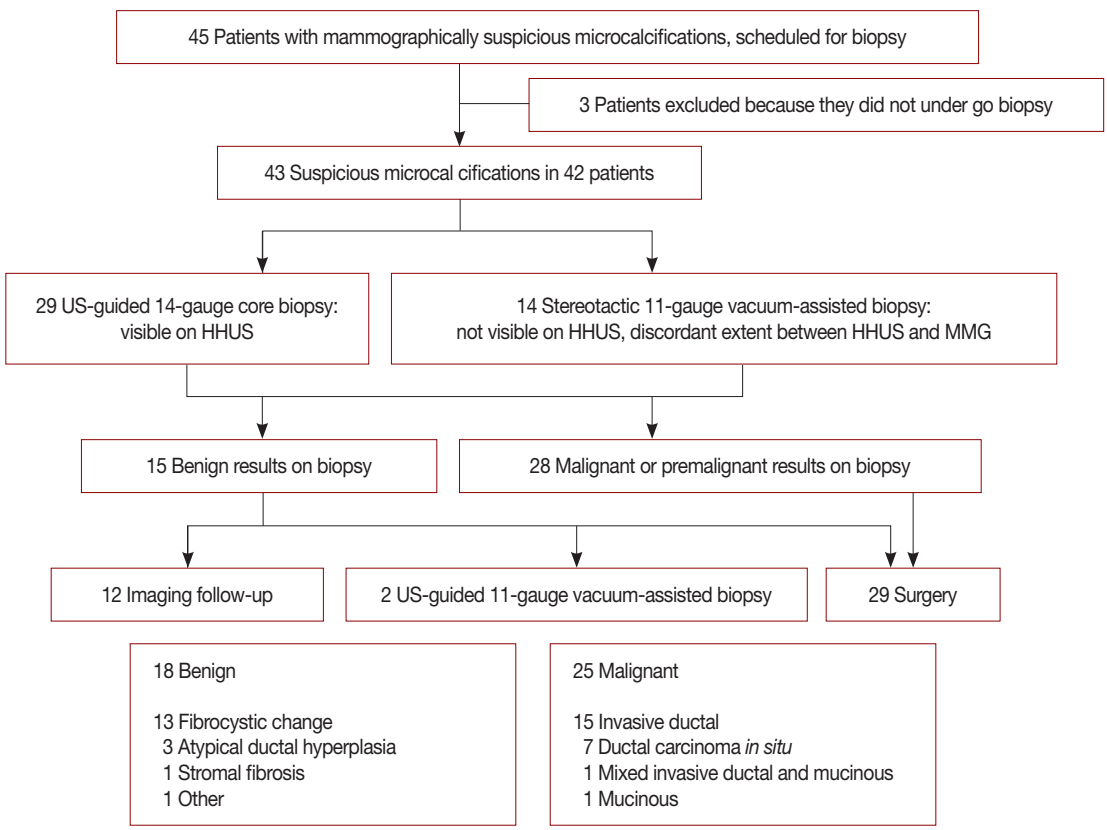

Figure 1. Flow chart shows the study population, inclusion and exclusion criteria, and pathologic findings. Three patients with benign results on biopsy underwent 11-gauge vacuum-assisted biopsy or surgical excision due to patient anxiety.
US = ultrasound; HHUS = handheld breast ultrasound; MMG = mammography.

https://doi.org/10.4048/jbc.2016.19.4.429

graphs were obtained to confirm the presence of representative microcalcifications in the tissue specimen. Additional core samples were obtained if a sufficient number of microcalcifications were not visualized in the tissue specimen. A radiopaque marker was not inserted after the biopsy procedure.

All patients underwent surgery with mammography-guided wire localization if malignancy or atypical ductal hyperplasia was diagnosed from the 14-gauge core needle or 11-gauge vacuum-assisted biopsy samples. In those cases, we considered the pathological results obtained from the surgical specimens to be the final diagnosis. One case of atypical ductal hyperplasia was confirmed to be invasive ductal carcinoma following surgical excision. Three patients with benign disease diagnosed by core needle biopsy underwent surgical excision or 11-gauge vacuum-assisted biopsy due to patient anxiety. No histologic underestimation was discovered in these patients. Follow-up imaging was performed on the remaining patients for 24 to 30 months.

Mammographic examinations and assessments

The standard craniocaudal and mediolateral oblique views were obtained using a Mammomat 3000 unit (Siemens Medical Solutions, Solna, Sweden) and a Lorad M3 mammography unit (Hologic Inc., Boston, USA). Lesion size was defined as the maximum diameter on either craniocaudal or mediolateral oblique images, and the presence of an associated mass or architectural distortion was analyzed on standard mammographic views. Spot compression and magnification images were also available for review in 15 of the 42 patients. The morphology, distribution, and final assessment categories of the microcalcifications and breast density were classified according to the American College of Radiology Breast Imaging Reporting and Data System (BI-RADS). Subcategories of category 4 were created according to the probability of malignancy: 3%–10% in 4a (low suspicion), 11%–50% in 4b (intermediate suspicion), and 51%–94% in 4c lesions (moderate suspicion). Mammographic breast densities were classified as follows: a, the breasts are almost entirely fatty; b, there are scattered areas of fibroglandular density; c, the breasts are heterogeneously dense, which may obscure small masses; d, the breast area extremely dense, which lowers the sensitivity of mammography.

Handheld breast ultrasound

HHUS examinations were performed by one of three radiologists (1, 8, and 10 years of experience with breast HHUS, respectively) with prior knowledge of the mammographic findings using a 7–15 MHz linear transducer (iU22 Ultrasound System; Philips Ultrasound, Bothell, USA) or a 6–14 MHz linear transducer (EUB-8500 Scanner; Hitachi Medical, Tokyo, Japan).

HHUS examinations focused on regions containing microcalcifications defined by their positions on a clock, distance from the nipple, and depth as determined by mammography. The radiologists assessed the visibility of the microcalcifications and the presence of associated masses or ductal changes. Lesions were considered to be microcalcifications when echogenic dots not traced to echogenic anatomic structures were discovered by HHUS in regions that had been previously identified by mammography.

Automated whole breast ultrasound

AWUS images were obtained using an ACUSON S2000 Automated Breast Volume Scanner (ABVS; Siemens Medical Solutions, Mountain View, USA) by one trained radiographer. The AWUS acquired 15.4×16.8×maximum 6-cm volume data sets of the breast in one sweep with a 5–14 MHz wide-aperture linear probe. The breast was initially scanned in the anterior-posterior view, which included the nipple and most parts of the breast with the patient in a supine position. The lateral and medial views, which mainly included the outer breast and the inner breast, were then scanned with the patient in an oblique position. After the acquisition of 3D volume data, it was automatically sent from the ACUSON S2000 ABVS to the workstation and reviewed in multiple orientations using a multi-planar reconstruction display. The images were displayed at a scan thickness of 1 mm without overlap.

Image review and data analysis for automated whole breast ultrasound

Two radiologists, who had 8 and 6 years of experience with breast imaging, respectively, analyzed all of the AWUS data in consensus. Each radiologist had more than 12 months of experience with AWUS prior to participating in this study. As one of the radiologists also performed the HHUS examinations, analysis of AWUS data was performed at 6-month intervals to avoid bias. After reviewing the mammographic images, the visibility of microcalcifications, associated masses, and ductal changes were assessed on the AWUS images. The radiologists focused on regions containing microcalcifications defined by using their positions with respect to a clock, distance from the nipple, and depth as determined by mammography. Lesions were considered to be microcalcifications when echogenic dots not traced to echogenic anatomic structures were discovered by AWUS in regions that had been previously identified by mammography. We did not assess the diagnostic performance of the two US modalities because it was difficult to characterize microcalcifications according to BI-RADS.

Statistical analyses

The detection rates of the mammographically identified microcalcifications by AWUS and HHUS were calculated. To determine whether detection by US was affected by pathology (benign vs. malignant lesions) or mammographic findings (size, shape, distribution, presence of an associated mass, BI-RADS category, and breast density), statistical analysis was performed using SAS version 9.1 (SAS Institute Inc., Cary, USA) and MedCalc® version 11.2.1.0 (MedCalc Software, Mariakerke, Belgium) software programs. We used Fisher exact test for categorical variables and the Mann-Whitney U-test for continuous variables. In addition, simple logistic regression was performed to identify the association between risk factors and dichotomous outcomes. A *p*-value of less than 0.05 was considered statistically significant.

Table 1. Mammographic features of 43 suspicious microcalcifications

Mammographic feature	Pathology		*p*-value
	Benign (n=18) No. (%)	Malignant (n=25) No. (%)	
Breast densities			0.407
a, b	5 (33.3)	10 (66.7)	
c, d	13 (46.4)	15 (53.6)	
Lesion extent (cm)*	1.3 (0.5–6.6)	2.0 (0.6–10.9)	0.232
Shape			<0.001
Punctate/round	4 (80.0)	1 (20.0)	
Amorphous	11 (68.7)	5 (31.3)	
Coarse heterogeneous	2 (66.7)	1 (33.3)	
Fine pleomorphic, linear, linear-branching	1 (5.3)	18 (94.7)	
Distribution			0.234
Regional	4 (40.0)	6 (60.0)	
Clustered	12 (52.2)	11 (47.8)	
Linear	0	0	
Segmental	2 (20.0)	8 (80.0)	
Associated findings			<0.001
None	16 (66.7)	8 (33.3)	
Mass	2 (11.1)	16 (88.9)	
Architectural distortion	0	1 (100.0)	
BI-RADS categories			<0.001
4a	14 (87.5)	2 (12.5)	
4b	4 (33.3)	8 (66.7)	
4c	0	8 (100.0)	
5	0	7 (100.0)	

BI-RADS=Breast Imaging Reporting and Data System.
*Median (range).

RESULTS

Of the 43 mammographically suspicious microcalcifications, 25 lesions (58.1%) were malignant (15 invasive ductal carcinomas, one mixed invasive ductal and mucinous carcinoma, one mucinous carcinoma, and seven ductal carcinoma *in situ* [DCIS]) and the remaining 18 (41.9%) were benign (three atypical ductal hyperplasia, 13 fibrocystic changes, one massive histiocytic infiltration with multinucleated giant cells, and one stromal fibrosis).

On mammograms, the lesion size varied from 0.5 to 10.9 cm. The size and breast density did not differ significantly between benign and malignant histology. The mammographic findings for the 43 lesions are summarized in Table 1.

Of the 43 lesions, 32 (74.4%) were detectable on AWUS and 31 (72.1%) were detectable on HHUS (Table 2). No significant differences were found in the detection rates between AWUS

Table 2. Comparison of detectability for suspicious microcalcifications between AWUS and HHUS

Pathology	No. of detections (detection rate)		*p*-value
	AWUS	HHUS	
Total (n=43)	32 (74.4)	31 (72.1)	0.998
Malignant (n=25)	24 (96.0)	24 (96.0)	>0.999
Benign (n=18)	8 (44.4)	7 (38.9)	0.997

AWUS=automated whole breast ultrasound; HHUS=handheld breast ultrasound.

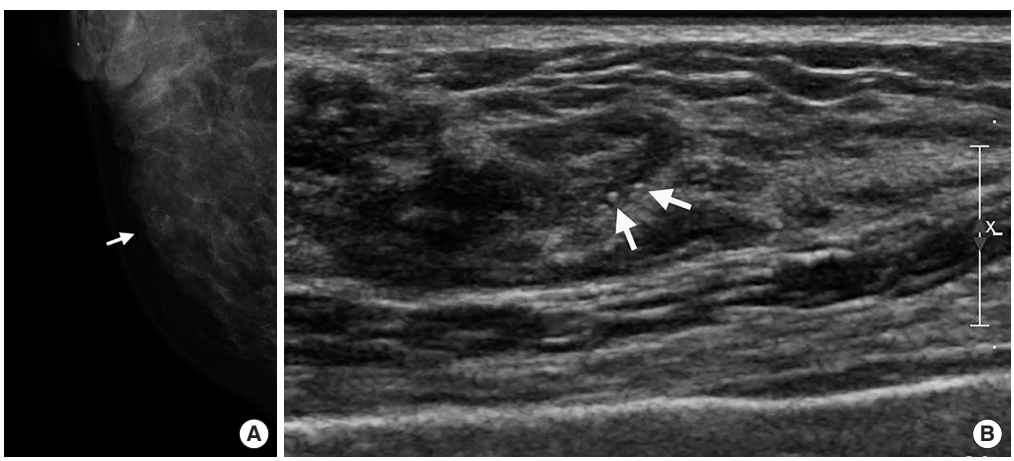

Figure 2. A 42-year-old woman with fibrocystic disease in the right breast. (A) Spot magnification mammogram shows grouped punctate microcalcifications in inner breast (arrow). (B) Handheld ultrasound (US) shows hyperechoic microcalcifications (arrows). These microcalcifications were not seen by automated whole breast US. This may be due to the lower resolution of automated whole breast US.

https://doi.org/10.4048/jbc.2016.19.4.429

(96% for malignant, 44.4% for benign) and HHUS (96% for malignant, 38.9% for benign, $p=0.998$). Among the two lesions detected by AWUS only and the one lesion detected by HHUS only, there was no malignancy. These three lesions appeared as hyperechoic dots in a hypoechoic parenchyma on either HHUS (Figure 2) or AWUS (Figure 3). Among the 10 lesions not detected by HHUS or AWUS, one was malignant. This lesion was identified as DCIS on histology and was visualized in the deep central portion of the breast by mammography and breast magnetic resonance imaging (Figure 4).

Using AWUS, malignant microcalcifications were more frequently visible than were benign microcalcifications ($p=0.003$) (Table 3). The detection rate was 86.7% (26/30) for lesions that were larger than 10 mm and only 46.2% (6/13) for lesions that were smaller than this ($p=0.009$). Lesions with fine pleomorphic or fine linear shapes (94.7%, 18/19) were more frequently visible than lesions with round, amorphous, or coarse heterogeneous shapes (58.3%, 14/24) ($p=0.021$). AWUS detected all 19 microcalcifications associated with masses or architectural distortions but only 13 of 24 (54.2%) lesions without associated abnormalities ($p=0.022$). In all 17 cases with invasive carcinoma, microcalcifications were observed within hypoechoic masses on AWUS. In six of the cases with DCIS, microcalcifications were observed within hypoechoic masses, abnormal parenchyma, or hypoechoic duct-like structures (Figure 5).

HHUS showed similar results to AWUS in the detection of mammographically suspicious microcalcifications (Table 4). Using HHUS, malignant microcalcifications were more frequently visible than benign microcalcifications ($p=0.001$).

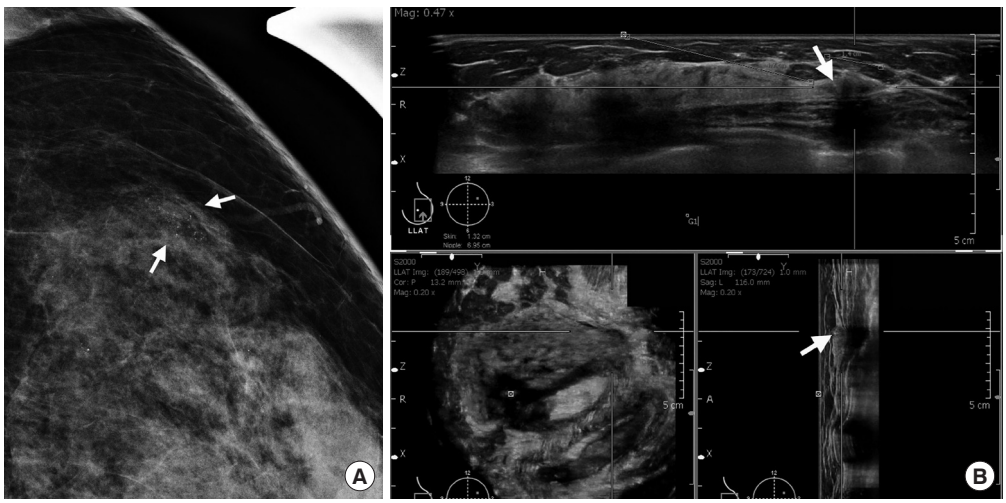

Figure 3. A 49-year-old woman with fibrocystic disease in the left breast. (A) Spot magnification mammogram shows grouped punctate or amorphous microcalcifications in outer breast (arrows). (B) Automated whole breast ultrasound (US) shows hyperechoic microcalcifications within the hypoechoic area (arrows). These microcalcifications were not detected by handheld US. This may be due to the operator dependency of handheld breast US.

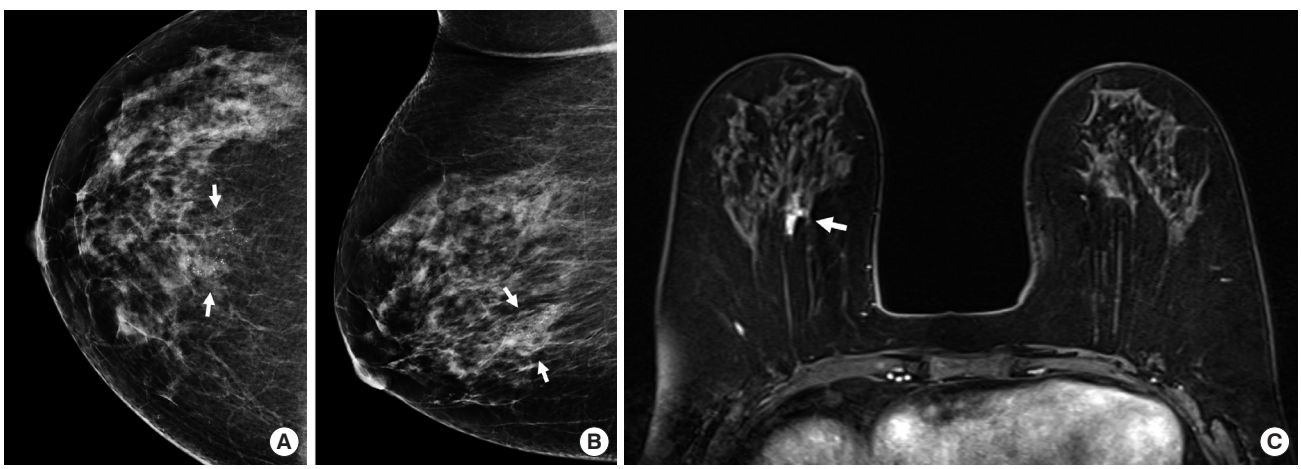

Figure 4. A 58-year-old woman with ductal carcinoma *in situ* in the right breast. (A, B) Craniocaudal and mediolateral oblique views of mammogram shows fine pleomorphic microcalcifications in deep central breast (arrows). (C) Axial T1-weighted contrast-enhanced magnetic resonance image shows an irregular enhancing mass in central posterior portion of right breast (arrow). These microcalcifications were not seen by hand held ultrasound (US) and automated whole breast US.

Table 3. Factors affecting the detectability of AWUS for mammographically suspicious microcalcifications

Pathologic and mammographic finding	AWUS		OR (95% CI)	*p*-value
	Not detected (n=11) No. (%)	Detected (n=32) No. (%)		
Pathology				0.003
Benign	10 (55.6)	8 (44.4)	1.000	
Malignant	1 (4.0)	24 (96.0)	30.000 (3.302–272.343)	
Extent (cm)				0.009
≤1	7 (53.8)	6 (46.2)	1.000	
>1	4 (13.3)	26 (86.7)	7.583 (1.666–34.520)	
Shape				0.021
Punctate/round, amorphous, coarse heterogeneous	10 (41.7)	14 (58.3)	1.000	
Fine pleomorphic, linear, linear branching	1 (5.3)	18 (94.7)	12.856 (1.466–112.701)	
Distribution				0.223
Regional, clustered	10 (30.3)	23 (69.7)	1.000	
Linear, segmental	1 (10.0)	9 (90.0)	3.911 (0.436–35.122)	
Associated findings				0.022
None	11 (45.8)	13 (54.2)	1.000	
Mass, architectural distortion	0	19 (100.0)	33.220 (1.671–660.447)	
BI-RADS categories				0.064
4a, 4b	10 (35.7)	18 (64.3)	1.000	
4c, 5	1 (6.7)	14 (93.3)	7.778 (0.887–68.189)	
Breast densities				0.905
a, b	4 (26.7)	11 (73.3)	1.000	
c, d	7 (25.0)	21 (75.0)	1.091 (0.261–4.553)	

AWUS=automated whole breast ultrasound; OR=odds ratio; CI=confidence interval; BI-RADS=Breast Imaging Reporting and Data System.

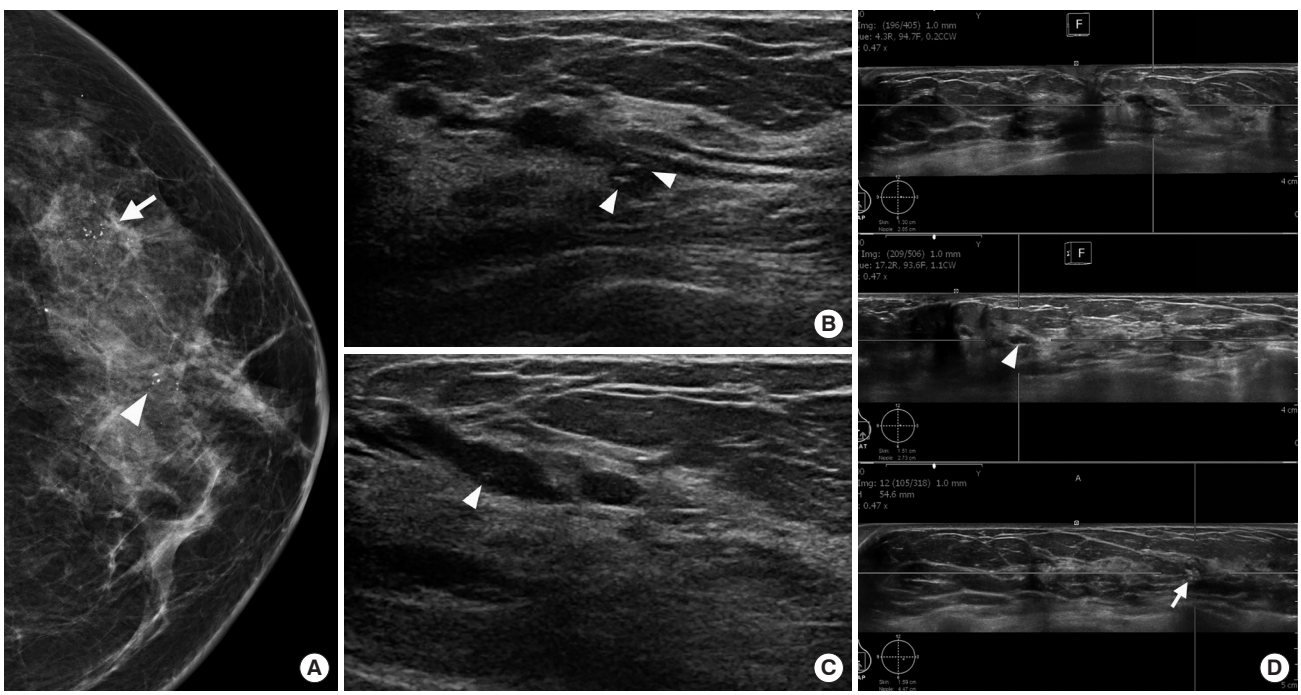

Figure 5. A 43-year-old woman with ductal carcinoma *in situ* in the left breast. (A) Craniocaudal view of mammogram shows segmental fine pleomorphic microcalcifications in central (arrowhead) and peripheral outer breast (arrow). (B, C) Handheld ultrasound (US) shows an intraductal hypoechoic mass with microcalcifications (arrowheads), which matched with central microcalcifications on mammogram. (D) Automated whole breast US shows segmental ductal dilatation with intraductal microcalcifications (arrowhead), which matched with central microcalcifications on mammogram. Grouped microcalcifications (arrow) in peripheral breast are found, which matched with peripheral microcalcifications on mammogram.

https://doi.org/10.4048/jbc.2016.19.4.429

Table 4. Factors affecting the detectability of HHUS for mammographically suspicious microcalcifications

Pathologic and mammographic finding	HHUS		OR (95% CI)	*p*-value
	Not detected (n=12) No. (%)	Detected (n=31) No. (%)		
Pathology				0.001
Benign	11 (61.6)	7 (38.9)	1.000	
Malignant	1 (40.0)	24 (96.0)	37.714 (4.123–344.993)	
Extent (cm)				0.017
≤1	7 (53.8)	6 (46.2)	1.000	
>1	5 (16.7)	25 (83.3)	5.833 (1.364–24.941)	
Shape				0.014
Punctate/round, amorphous, coarse heterogeneous	11 (45.8)	13 (54.2)	1.000	
Fine pleomorphic, linear, linear branching	1 (5.3)	18 (94.7)	15.228 (1.743–133.065)	
Distribution				0.528
Regional, clustered	10 (30.3)	23 (69.7)	1.000	
Linear, segmental	2 (20.0)	8 (80.0)	1.739 (0.312–9.694)	
Associated findings				0.016
None	12 (50.0)	12 (50.0)	1.000	
Mass, architectural distortion	0	19 (100.0)	39.020 (1.963–775.810)	
BI-RADS categories				0.046
4a, 4b	11 (39.3)	17 (60.7)	1.000	
4c, 5	1 (6.7)	14 (93.3)	9.059 (1.039–79.010)	
Breast densities				0.894
a, b	4 (26.7)	11 (73.3)	1.000	
c, d	8 (28.6)	20 (71.4)	0.909 (0.222–3.715)	

HHUS=handheld breast ultrasound; OR=odds ratio; CI=confidence interval; BI-RADS=Breast Imaging Reporting and Data System.

The detection rate was higher for lesions that were larger than 10 mm (83.3%) than for lesions that were smaller (46.2%, $p=0.017$). The detection rate was also higher for lesions with fine pleomorphic or fine linear shapes (94.7%) than for lesions with round, amorphous, or coarse heterogeneous shapes (54.2%, $p=0.014$). Likewise, the detection rate was higher for lesions associated with masses or architectural distortions (100%) than it was for lesions without associated abnormalities (50.0%, $p=0.022$). Finally, lesions categorized as BI-RADS 4c or 5 (93.3%) were more frequently detected than lesions categorized as BI-RADS 4a or 4b by mammography (60.7%, $p=0.046$).

DISCUSSION

The objective of this study was to examine the ability of AWUS to detect suspicious microcalcifications initially identified by mammography and to characterize the lesion variables that affect the detectability of AWUS as compared to HHUS. In this prospective evaluation of 43 cases, we showed that the detectability of AWUS was comparable to that of HHUS. Using AWUS, 74.4% of mammographically suspicious microcalcifications were identified (96% of malignant microcalcifications and 44.4% of benign microcalcifications). Using HHUS, 72.1% of the microcalcifications were identified (96.0% of malignant microcalcifications and 38.9% of benign microcalcifications). These findings are consistent with previous studies evaluating HHUS, in which a 69% to 100% detection rate for malignant microcalcifications and a 23% to 66% detection rate for benign microcalcifications was described [7,8,12].

Both AWUS and HHUS identified malignant microcalcifications more frequently than benign microcalcifications. It is likely that the hypoechoic backgrounds of the masses or duct-like structures increased the conspicuity and detectability of the echogenic microcalcifications. These US findings are similar to those described previously [7, 8,11,12]. In our study, one DCIS lesion located deep in the central portion of the breast was not detected by either AWUS or HHUS. Sonographic posterior acoustic shadowing beneath the nipple may have influenced the detectability of the lesion. In contrast to malignant lesions, microcalcifications associated with benign histology were visible in only eight of 18 cases. Microcalcifications were detected within hypoechoic masses, anechoic cysts, and normal parenchyma using AWUS, similar to lesions described in a previous study [7]. The microcalcifications that were not visible on AWUS did not have associated masses or cysts. This discrepancy is believed to be due to a lack of contrast between normal parenchyma with hyperechoic fibrous

structures and the microcalcifications.

In our study population, a case with a benign lesion, which displayed discrete hyperechoic dots within normal parenchyma on HHUS, was not detected on AWUS. This may be due to the lower resolution of AWUS resulting from the use of a lower frequency transducer and wider focal zone. In contrast, two benign lesions detected by AWUS were not visible using HHUS. This may be due to the operator dependency of HHUS.

In our study, the mammographic features of the microcalcifications that predicted their detectability by AWUS were a larger size (> 10 mm) and a fine pleomorphic or linear shape. The factors affecting the detectability of AWUS were similar to those affecting the detectability of HHUS for mammographically suspicious microcalcifications. These results are consistent those of a previous study that found that the visibility of clustered microcalcifications on HHUS was much higher in cases with malignant microcalcifications, particularly for those larger than 10 mm [7].

Our study had some limitations. First, only a small number of lesions were evaluated, and these had been previously identified by mammography; this is not representative of the general population. Further studies that include larger numbers of patients undergoing routine screening for breast cancer are required. Second, for lesions that were not visible by US and were instead confirmed by stereotactic biopsy, we considered their size, clock-wise location, and depth of the lesions and made an effort to correlate the findings between US and mammography. Finally, we did not consider the possibility of underestimation of pathologic results by US-guided 14-gauge core needle biopsy and stereotactic 11-gauge vacuum-assisted biopsy. However, 15 lesions diagnosed as benign by US-guided 14-gauge core needle biopsy and stereotactic 11-gauge vacuum-assisted biopsy showed no significant changes at the 24 to 30 months follow-up visits.

In conclusion, the detectability of AWUS was comparable to that of HHUS for mammographically suspicious microcalcifications. The detectability of AWUS is much higher for malignant microcalcifications, particularly those larger than 10 mm, having a suspicious morphology, and associated with masses or architectural distortion on mammography. Therefore, for highly suspicious microcalcifications, AWUS might be helpful to predict the feasibility of US-guided percutaneous procedures.

CONFLICT OF INTEREST

The authors declare that they have no competing interests.

ACKNOWLEDGMENTS

We thank the Clinical Research Coordinating Center at the Catholic University of Korea for statistical analyses.

REFERENCES

1. Sickles EA. Breast calcifications: mammographic evaluation. Radiology 1986;160:289-93.
2. Sickles EA. Mammographic features of 300 consecutive nonpalpable breast cancers. AJR Am J Roentgenol 1986;146:661-3.
3. Ciatto S, Cataliotti L, Distante V. Nonpalpable lesions detected with mammography: review of 512 consecutive cases. Radiology 1987;165:99-102.
4. Meyer JE, Kopans DB, Stomper PC, Lindfors KK. Occult breast abnormalities: percutaneous preoperative needle localization. Radiology 1984;150:335-7.
5. Meyer JE, Eberlein TJ, Stomper PC, Sonnenfeld MR. Biopsy of occult breast lesions: analysis of 1261 abnormalities. JAMA 1990;263:2341-3.
6. Orel SG, Kay N, Reynolds C, Sullivan DC. BI-RADS categorization as a predictor of malignancy. Radiology 1999;211:845-50.
7. Moon WK, Im JG, Koh YH, Noh DY, Park IA. US of mammographically detected clustered microcalcifications. Radiology 2000;217:849-54.
8. Gufler H, Buitrago-Téllez CH, Madjar H, Allmann KH, Uhl M, Rohr-Reyes A. Ultrasound demonstration of mammographically detected microcalcifications. Acta Radiol 2000;41:217-21.
9. Hashimoto BE, Kramer DJ, Picozzi VJ. High detection rate of breast ductal carcinoma in situ calcifications on mammographically directed high-resolution sonography. J Ultrasound Med 2001;20:501-8.
10. Cheung YC, Wan YL, Chen SC, Lui KW, Ng SH, Yeow KM, et al. Sonographic evaluation of mammographically detected microcalcifications without a mass prior to stereotactic core needle biopsy. J Clin Ultrasound 2002;30:323-31.
11. Soo MS, Baker JA, Rosen EL, Vo TT. Sonographically guided biopsy of suspicious microcalcifications of the breast: a pilot study. AJR Am J Roentgenol 2002;178:1007-15.
12. Soo MS, Baker JA, Rosen EL. Sonographic detection and sonographically guided biopsy of breast microcalcifications. AJR Am J Roentgenol 2003;180:941-8.
13. Shipley JA, Duck FA, Goddard DA, Hillman MR, Halliwell M, Jones MG, et al. Automated quantitative volumetric breast ultrasound data-acquisition system. Ultrasound Med Biol 2005;31:905-17.
14. Tozaki M, Fukuma E. Accuracy of determining preoperative cancer extent measured by automated breast ultrasonography. Jpn J Radiol 2010;28:771-3.
15. Kim SH, Kang BJ, Choi BG, Choi JJ, Lee JH, Song BJ, et al. Radiologists' performance for detecting lesions and the interobserver variability of automated whole breast ultrasound. Korean J Radiol 2013;14:154-63.
16. Shin HJ, Kim HH, Cha JH, Park JH, Lee KE, Kim JH. Automated ultrasound of the breast for diagnosis: interobserver agreement on lesion detection and characterization. AJR Am J Roentgenol 2011;197:747-54.
17. Lin X, Wang J, Han F, Fu J, Li A. Analysis of eighty-one cases with breast

 https://doi.org/10.4048/jbc.2016.19.4.429

lesions using automated breast volume scanner and comparison with handheld ultrasound. Eur J Radiol 2012;81:873-8.
18. Wang HY, Jiang YX, Zhu QL, Zhang J, Dai Q, Liu H, et al. Differentiation of benign and malignant breast lesions: a comparison between automatically generated breast volume scans and handheld ultrasound examinations. Eur J Radiol 2012;81:3190-200.
19. Kotsianos-Hermle D, Hiltawsky KM, Wirth S, Fischer T, Friese K, Reiser M. Analysis of 107 breast lesions with automated 3D ultrasound and comparison with mammography and manual ultrasound. Eur J Radiol 2009;71:109-15.
20. Kotsianos-Hermle D, Wirth S, Fischer T, Hiltawsky KM, Reiser M. First clinical use of a standardized three-dimensional ultrasound for breast imaging. Eur J Radiol 2009;71:102-8.
21. An YY, Kim SH, Kang BJ. The image quality and lesion characterization of breast using automated whole-breast ultrasound: a comparison with handheld ultrasound. Eur J Radiol 2015;84:1232-5.